Hemodynamic responses following brief breath-holding and visual stimulation reconcile the vascular compliance and sustained oxygen metabolism origins for the BOLD post-stimulus undershoot in human brain

J. Hua[1], R. Stevens[1], A. J. Huang[1], J. J. Pekar[1], and P. C. van Zijl[1]
[1]Department of Radiology, The Johns Hopkins University, Baltimore, MD, United States

Introduction: The well-known BOLD post-stimulus undershoot has been attributed to two possible origins: (i) delayed vascular compliance based on delayed cerebral blood volume (CBV) recovery (1,2) or undershoot in cerebral blood flow (CBF) (3) with recovery of oxygen metabolism; (ii) sustained oxygen metabolism with speedy CBV and CBF recovery after stimulus cessation (4,5). Recently, high-resolution fMRI studies in cat brain revealed that both mechanisms may affect the BOLD undershoot in middle cortical layers whereas the metabolic origin may be the reigning factor in pial vessels located close to the cortical surface (6,7). While the BOLD undershoot is consistently observed after focal neuronal stimulation, it is absent following brief global hypercapnic challenges (8), which serves as a unique model for further investigation of its mechanism. In this study, we employed multi-modality fMRI techniques to monitor the transient responses of BOLD, CBF, total CBV and arterial CBV (CBV_a) *in vivo* in human visual cortex after breath-hold and visual stimulation, respectively, seeking to clarify which mechanism dominates the BOLD undershoot, and, if both contribute, what their relative contribution is.

Methods: Eleven subjects were scanned on a 3T Philips MRI scanner using 8 pseudo-randomized fMRI sessions for each participant including BOLD, CBF, CBV and CBV_a measurements during a visual task (4 blocks of 55s cross-hair fixation+15s 8Hz flashing checkerboard) and a breath-hold task (4 blocks of 50s normal breathing+5s exhaling+15s breath-holding), *respectively*. Common parameters: voxel=3x3x3mm^3, single slice centered on calcarine fissure, single shot turbo spin echo (TSE) readout, TE=6ms, SENSE=2.5. *CBF*: The transfer-insensitive-labeling-technique (TILT) ASL technique (9) was employed: TR/TI=2.5s/1.6s, label thickness=80mm, label/slice gap=12.5 mm, crushing gradients V_{enc}=3cm/s, b=1.7s/mm^2. *CBV*: long-TR VASO MRI (10) sensitized to total ΔCBV: TR/TI=5s/1054ms. *CBV_a*: A recently developed iVASO technique (11) was used, in which a non-selective inversion is followed by a slab-selective inversion that flips back the water spins within the imaging slice and superior brain region. By choosing a proper TI that is comparable to the mean arterial transit time in human visual cortex, the inverted blood water spins will be nulled by the time they perfuse the arterial compartment but before reaching capillaries and venules, allowing assessment of arterial CBV effects. TR/TI=2.5s/811ms, flip-back slab thickness=80mm, flip-back/slice gap=10mm. *BOLD*: gradient echo (GE) single shot echo-planar-imaging (EPI) (TR/TE/flip angle=2.5s/45ms/85°), crushing gradients (b=60s/mm^2) to suppress large vessel signals, 15 slices, only the center slice that aligned with other single slice location was processed. *Analysis*: All images were co-registered and baseline drift was corrected. A two-tailed Z-test was engaged for activation detection (Z-score>2.5, cluster>4, SNR>20). Only voxels activated in all eight scans were analyzed. ΔCBV and ΔCBV_a were quantified with VASO (10) and iVASO (11) theories, respectively. $CMRO_2$ dynamics was estimated using both the models from Lu et al. (5) and Davis et al. (12). The Lu model was slightly modified to incorporate CBV_a dynamics, instead of assuming CBV_a/CBV=30% during both baseline and activation. In the Davis model, measured ΔCBV from breath-hold and visual stimulation was used, rather than estimating it from ΔCBF with Grubb's empirical equation.

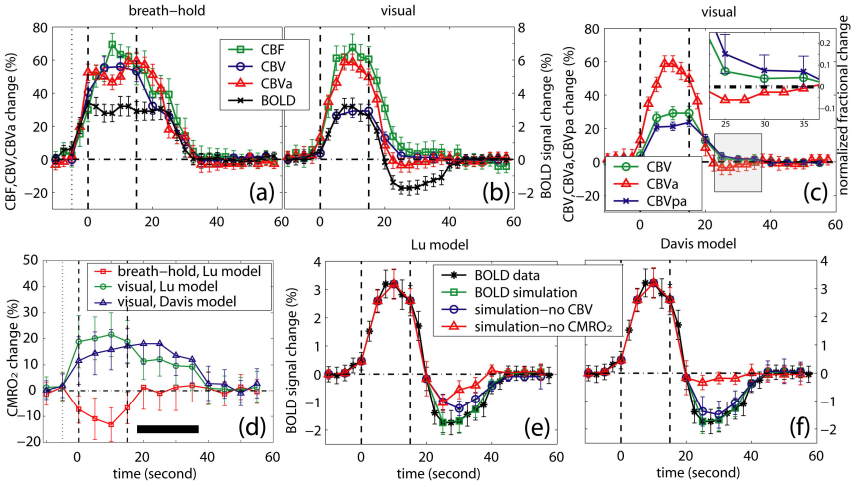

Results & Discussion: The average time courses of relative changes (ΔS/S) in CBF, CBV, CBV_a and BOLD signal (n=10) are displayed in Figs. a,b for breath-hold and visual tasks, respectively. The BOLD undershoot is evident after visual stimulation but absent following breath-hold. All four time courses returned to baseline within about 20s after breath-hold ends. For visual stimulation, CBV_a returned to baseline faster than CBF and CBV (P<0.01); no significant difference between CBF and CBV recovery was found (P>0.1). CBF, CBV and CBV_a were at baseline during most of the BOLD undershoot. The post-arterial volume change (ΔCBV_{pa}) inferred from ΔCBV and ΔCBV_a, shown in Fig. c, was slightly elevated (2.4+/-1.8%, P<0.05) during the BOLD undershoot. This finding indicates that delayed CBV (2), especially CBV_{pa} (3), recovery after stimulus cessation partially contributes to the BOLD undershoot. Note that because of the R_2^* difference in tissue, arterial and post-arterial blood, a decrease in CBV_a and an increase in CBV_{pa} would both diminish the overall BOLD signal, which may partly contribute to the undershoot after visual stimulation. In contrast, after breath-hold, when CBV_a and CBV_{pa} recovered equivalently, their effects on BOLD signal largely cancel out, which may partly explain the absence of a BOLD undershoot. Fig. d shows the $CMRO_2$ changes in both tasks calculated with the Lu model and Davis model. Note that as the Davis model needs to use BOLD, CBF and CBV measurements during breath-hold for estimating the calibration factor M, it can only calculate $\Delta CMRO_2$ for the visual task. After breath-hold ends, $CMRO_2$ was at baseline (0.9+/-7.7%) whereas $CMRO_2$ remained elevated (P<0.01) for 20-25s after visual stimulation is stopped, which supports the hypothesis that sustained oxygen consumption have a large influence on the BOLD undershoot (5). These results imply that the BOLD undershoot is an aggregate consequence of both delayed CBV_{pa} recovery and enduring oxygen metabolism. To evaluate relative contributions from both origins, simulations were performed using the Lu model (Fig. e) and Davis model (Fig. f) to predict BOLD ΔS/S in the visual task under different assumptions. First, BOLD ΔS/S was simulated with all original measurements and matched with the measured BOLD ΔS/S (undershoot amplitude 1.26+/-0.31%) to verify the accuracy of calculation. Second, BOLD ΔS/S was calculated assuming total CBV to be at baseline (ΔCBV =0) during the BOLD undershoot. The amplitude of BOLD undershoot decreased to 0.89+/-0.25% and 1.07+/-0.33%, indicating 20+/-16% and 13+/-23% contribution from delayed CBV_{pa} return, as predicted by the Lu model and Davis model, respectively. Finally, simulations were performed with original measurements of CBF, CBV and CBV_a, but $\Delta CMRO_2$ during the BOLD undershoot artificially set to zero. The amplitude of resulting BOLD undershoot declined to 0.46+/-0.27% and 0.17+/-0.25%, indicating 79+/-19% and 86+/-23% contribution from sustained metabolism, as predicted by the Lu model and Davis model, respectively. Note that the relative contribution from $CMRO_2$ calculated by the Davis model were slightly higher (P<0.1) than that from the Lu model, which is largely due to the fact that ΔCBV is used to approximate ΔCBV_{pa} and the signal contribution from ΔCBV_a (R_2^* difference) is omitted in the Davis model.

Conclusion: Our results show that following visual stimulus cessation, CBV_a quickly returned to baseline while CBV_{pa} persisted and $CMRO_2$ remained substantially elevated for the duration of BOLD undershoot. On the other hand, after breath-hold ends, no BOLD undershoot, elevated CBV_{pa} and $CMRO_2$ were observed. These data suggest that both elevated CBV_{pa} and continued oxygen metabolism affect the undershoot, with contributions estimated as 20+/-16% and 79+/-19%, respectively, under our experimental conditions.

Grant support: P41 RR15241 (NCRR/NIH), R01 EB004130 (NIBIB/NIH).
(1)Buxton, RB, et al. MRM 1998;39:855.(2)Mandeville, JB, et al. JCBFM 1999;19:679.(3)Chen, JJ, et al. NeuroImage 2009;46:559.(4)Frahm, J, et al. MRM 1996;35:143.(5)Lu, H, et al. JCBFM 2004;24:764.(6)Yacoub, E, et al. JCBFM 2006;26:634.(7)Zhao, F, et al. NeuroImage 2007;34:1084.(8)Donahue, MJ, et al. JCBFM 2009;29:176.(9)Golay, X, et al. JMRI 1999;9:454.(10)Lu, H, et al. MRM 2003;50:263.(11)Hua, J, et al. ISMRM 2009;178.(12)Davis, TL, et al. PNAS 1998;95:1834.